

1 **Muscle RANK is a key regulator of calcium storage, SERCA**  
2 **activity, and function of fast-twitch skeletal muscles**  
3

4 Sébastien S. Dufresne<sup>1\*</sup>, Nicolas A. Dumont<sup>1\*</sup>, Antoine Boulanger-Piette<sup>1</sup>, Val A. Fajardo<sup>2</sup>,  
5 Daniel Gamu<sup>2</sup>, Sandrine-Auréliè Kake-Guena<sup>3</sup>, Rares Ovidiu David<sup>1</sup>, Patrice Bouchard<sup>1</sup>,  
6 Éliane Lavergne<sup>1</sup>, Josef M. Penninger<sup>4</sup>, Paul C. Pape<sup>3</sup>, A. Russell Tupling<sup>2</sup> and Jérôme  
7 Frenette<sup>1,5</sup>

8 <sup>1</sup> Centre Hospitalier Universitaire de Québec–Centre de Recherche du Centre Hospitalier de  
9 l’Université Laval (CHUQ-CRCHUL), Université Laval, Quebec City, QC, Canada G1V  
10 4G2

11 <sup>2</sup> Department of Kinesiology, University of Waterloo, Waterloo, Ontario, Canada N2L 3G1

12 <sup>3</sup> Département de physiologie et biophysique, Université de Sherbrooke Faculté de Médecine  
13 et des Sciences de la Santé, Sherbrooke, Québec, Canada J1H 5N4

14 <sup>4</sup> IMBA, Institute of Molecular Biotechnology of the Austrian Academy of Sciences, 1030  
15 Vienna, Austria

16 <sup>5</sup> Département de Réadaptation, Faculté de Médecine, Université Laval, Quebec City, QC,  
17 Canada G1V 4G2

18 \*These authors contributed equally to this work  
19

20 **Running head:** Rank is a novel calcium regulator in skeletal muscle  
21

22 **Keywords:** RANK, skeletal muscle, SERCA  
23  
24

25 Corresponding author: Jérôme Frenette PT, Ph.D

26 CHUQ-CRCHUL

27 2705 boulevard Laurier, RC-9500

28 Quebec City, QC, Canada G1V 4G2

29 Phone: (418) 656-4141, ext. 47779

30 Fax: (418) 654-2145

31 E-mail: [jerome.frenette@crchul.ulaval.ca](mailto:jerome.frenette@crchul.ulaval.ca)

32

33

34

35

36

37

38

39

40

41

42

43

44

45

46

47

48

49

50

51 **Abstract**

52

53 Receptor-activator of nuclear factor kB (RANK), its ligand RANKL and the soluble decoy  
54 receptor osteoprotegerin (OPG) are the key regulators of osteoclast differentiation and bone  
55 remodeling. Here we show that RANK is also expressed in fully differentiated myotubes and  
56 skeletal muscle. Muscle RANK deletion (*RANK<sup>zmko</sup>*) has inotropic effects in denervated, but  
57 not in sham, extensor digitorum longus (EDL) muscles preventing the loss of maximum  
58 specific force while promoting muscle atrophy, fatigability and increased proportion of fast-  
59 twitch fibers. In denervated EDL muscles, RANK deletion markedly increased stromal  
60 interaction molecule 1 (Stim1) content, a calcium sensor, and altered activity of the  
61 sarco(endo)plasmic reticulum  $\text{Ca}^{2+}$  ATPase (SERCA) modulating  $\text{Ca}^{2+}$  storage. Muscle  
62 RANK deletion had no significant effects on the sham or denervated slow-twitch soleus (Sol)  
63 muscles. These data identify a novel role for RANK as a key regulator of calcium storage and  
64 SERCA activity, ultimately affecting denervated skeletal muscle function.

65

66

67

68

69

70 **Introduction**

71 Receptor-activator of nuclear factor kB ligand (RANKL), the membrane receptor RANK  
72 and the soluble decoy receptor osteoprotegerin (OPG) are members of the tumor necrosis  
73 factor (TNF) superfamily that regulate bone remodelling (26, 29). RANK/RANKL  
74 interaction activates  $\text{Ca}^{2+}$ -dependent and NF-kB signalling pathways, which affect osteoclast  
75 differentiation, activation and survival (29). The third protagonist, OPG, binds to RANKL  
76 and inhibits the RANK/RANKL interaction and subsequent osteoclastogenesis (46, 55). In  
77 addition to bone, RANK/RANKL has been detected in other tissues such as thymus, heart,  
78 kidney, liver, brain, blood vessels and skeletal muscles (17, 32, 51). The RANK/RANKL  
79 pathway is known to be involved in a variety of physiological and pathological conditions  
80 such as lymph-node organogenesis, formation of lactating mammary gland, breast cancer,  
81 central thermoregulation, T-cell/dendritic cell communication, vascular calcification, and  
82 bone metastasis (18, 36, 38, 41, 45).

83

84 Muscle hypertrophy/atrophy and gain/loss of bone mineral density occur in parallel in  
85 many physiological or pathological conditions and endocrine, mechanical factors,  
86 inflammatory and nutritional states affect simultaneously skeletal muscle and bone  
87 metabolism (3, 4, 16, 22, 39). These observations are consistent with the view that skeletal  
88 muscle and bone share common cell signalling pathways. For example, the Wnt/ $\beta$ -catenin  
89 signalling pathway is a major regulator of bone mass and muscle development and growth  
90 (24). Conditional deletion of *Ctnnb1* gene in osteocytes, which encodes for  $\beta$ -catenin, leads  
91 to impaired bone maturation and mineralization with increased RANKL:OPG ratio (27). In  
92 bone, RANKL/RANK interactions activate tumour necrosis factor receptor-associated factors  
93 6 (TRAF-6), which subsequently induces the activation of downstream signalling molecules  
94 and intracellular calcium concentration ( $[\text{Ca}^{2+}]_i$ ) oscillations (53). The ATP-dependent  $\text{Ca}^{2+}$

95 pump, sarco(endo)plasmic reticulum  $\text{Ca}^{2+}$ ATPase (SERCA), is essential for  $[\text{Ca}^{2+}]_i$   
96 oscillations and plays a critical role in osteoclastogenesis (54). Moreover, it has been shown  
97 that TRAF-6 is required for functional bone resorption and muscle-specific TRAF-6 deletion  
98 preserves function and reduces atrophy in a model of muscle wasting indicating that TRAF-6  
99 is an important regulator of both bone and muscle masses (19, 49, 50). Thus, common  
100 signalling pathways are emerging to explain the synchronicity between bone and skeletal  
101 muscle physiology and pathophysiology.

102

103 Muscle contraction involves the depolarization of the transverse-tubular (t) system, which  
104 activates dihydropyridine receptors (DHPRs) opening ryanodine receptor/ $\text{Ca}^{2+}$  release  
105 channels (RYR1) in the sarcoplasmic reticulum (SR) membrane. This results in the rapid  
106 influx of  $\text{Ca}^{2+}$  into the cytoplasm through RYR1 and binding of  $\text{Ca}^{2+}$  ions to troponin C  
107 causing the formation of actin-myosin cross-bridges and force development (34). Calcium  
108 reuptake in the SR is a tightly control mechanism mediated almost exclusively by SERCA-1a  
109 in fast-twitch fibers and SERCA-2a in slow-twitch fibers. The regulation of  $\text{Ca}^{2+}$  is also  
110 implicated in other physiological processes such as the maintenance and adaptation of muscle  
111 phenotypes (7, 40), while chronic rise in  $[\text{Ca}^{2+}]_i$  is associated with different pathological  
112 states including muscle dystrophy (1) and the triggering of apoptotic processes (12, 42).  
113 Therefore, the appropriate regulation of  $[\text{Ca}^{2+}]_i$  is a requirement for proper cell function,  
114 phenotype and survival.

115

116 We recently reported that OPG treatments protect against muscular dystrophy suggesting a  
117 potential role for RANK/RANKL/OPG pathway in muscle disease. In addition, muscle  
118 specific TRAF-6 deletion prevented muscle atrophy and decreased the expression of  
119 ubiquitin-proteasome components in models of denervation or starvation (28, 50). In the

120 present study, we hypothesized that muscle RANK, a receptor upstream of TRAF-6, is an  
121 important regulator of denervated muscle function. We report that RANK/RANKL regulates  
122 Ca<sup>2+</sup> storage, function and phenotype, confirming a role for RANK in denervated skeletal  
123 muscles.  
124

125 **Material & Methods**

126

127 **Ethical Approval:** All procedures were approved by the Université Laval Research Center  
128 Animal Care and Use Committee based on Canadian Council on Animal Care guidelines.

129

130 **Animals:** Mice carrying the RANK<sup>floxed</sup> or RANK<sup>del</sup> alleles and muscle creatine kinase-Cre  
131 (mck-Cre) mice were backcrossed five times to a C57BL/10J background before generating a  
132 specific RANK skeletal muscle deletion, the mck-Cre RANK<sup>del/floxed</sup>, hereafter named  
133 Rank<sup>mko</sup> mice (18). RANK<sup>mko</sup> mice are viable, healthy and appeared indistinguishable from  
134 control RANK<sup>floxed/floxed</sup> mice that do not carry the Cre recombinase, hereafter named  
135 RANK<sup>f/f</sup> mice. Male wild-type (C57BL/10J) mice were purchased from the Jackson  
136 Laboratory and bred at our animal facility. Mice were screened for the desired genotype by  
137 PCR analysis. Food and water were provided ad libitum. At the end of the different  
138 experimental procedures, the mice were euthanized by cervical dislocation under anaesthesia.

139

140 **Denervation:** Sciatic denervation was performed under anaesthesia with isoflurane  
141 inhalation on adult mice aged between 12-18 weeks. Briefly, the hindlimbs were shaved and  
142 a small 0.5-cm incision was made proximal to the hip on the lateral side of the leg to expose  
143 and section a 3-5 mm piece of the sciatic nerve. The wounds were then closed with surgical  
144 sutures. The same surgery procedures were executed without sciatic denervation for sham  
145 mice. Mice were euthanized 14 days after sham or denervation procedures. Animals without  
146 surgical procedures were used as control mice.

147

148 **Cell culture:** C2C12 myoblasts (ATCC) were cultured in high glucose DMEM (HyClone)  
149 supplemented with 10% FBS (HyClone) and 1% antibiotic-antimycotic (Life Technologies)

150 in 5% CO<sub>2</sub> and at 37°C. When the myoblasts reached 90% confluence, the medium was  
151 replaced by high glucose DMEM containing 1% FBS for 5 days to allow the myoblasts to  
152 differentiate into myotubes (11).

153

154 **Genomic DNA for genotyping:** Genomic DNA from mouse tail tissue samples was isolated  
155 and amplified by PCR. RANK, cre, and dystrophin was identified by isolating genomic DNA  
156 from tail tissue and screening for the mutation or presence of the transgene by PCR. To detect  
157 *delta*, *flox* and *wild-type* alleles primers used were p87, p88 and p105. Conditions : 94 °C 2  
158 min, 40 cycles of (94 °C 30 s, 60 °C 20 s, 72 °C 1 min) and 72 °C 4 min. To detect the  
159 presence of the *mck-cre* primers used were ALP 130 and ALP 131. Conditions : 94 °C 2 min,  
160 40 cycles of (94 °C 30 s, 58 °C 10 s, 72 °C 1 min) and 72 °C 4 min. To detect *mdx* allele  
161 primers used were p9427 and p259E. Conditions : 94 °C 3 min, 45 cycles of (94 °C 30 s, 57  
162 °C 30 s, 72 °C 20 s) and 72 °C 10 min.

163 **Isometric contractile properties:** Mice were injected with buprenorphine (i.p. 0.1 mg/kg)  
164 and anesthetised with pentobarbital sodium (i.p. 50 mg/kg) 15 min later. Mice were weighed  
165 and the soleus (Sol) and extensor digitorum longus (EDL) muscles were carefully dissected,  
166 attached to an electrode and a force sensor (305B-LR, Aurora Scientific, Inc.) to assess  
167 contractile properties as described previously (9, 44). Muscle fatigability was examined by  
168 stimulating muscle for 200 ms every second at 50 Hz until muscles lost 30% (Sol) or 50%  
169 (EDL) of their initial force. Lastly, muscle length was measured, tendons were removed and  
170 muscles weighed for calculation of muscle cross-sectional area and specific force (13).  
171 Functional measurements were analyzed with the Dynamic Muscle Data Analysis software  
172 (Aurora Scientific, Inc.).

173

174 **Immunohistochemistry:** Transversal Sol and EDL muscle sections (10 µm) were cut (Leica



175 Microsystems CM1850, Nussloch, Germany) in duplicate from the proximal and distal  
176 portions of the muscles. Sections were incubated overnight at 4°C with the following primary  
177 antibodies: anti-SERCA1a (Abcam), anti-SERCA2a (Abcam), anti-MyHC I (Novus  
178 Biological), anti-MyHC IIA (SC-71, DSHB), anti-MyHC IIB (BF-F3, DSHB), anti-MyHC  
179 IIX (6H1, DSHB), anti-dystrophin (NCL-Dys1, Vector Laboratories) and anti-RANK (R&D  
180 Systems). Pan-MyHC II was obtained by combining three antibodies: anti-MyHC IIA, anti-  
181 MyHC IIB and anti-MyHC IIX (DSHB). Fiber-type differentiation by myosin  
182 immunohistochemical was performed as described by Schiaffino et al. (43). Biotinylated  
183 secondary antibodies for immunohistochemistry were purchased from Vector Laboratories  
184 and Alexa Fluor® secondary antibodies from Invitrogen. The localization of RANK and  
185 dystrophin in the sarcolemmal membrane of skeletal muscles was determined by confocal  
186 microscopy. Briefly, confocal series were acquired using a Quorum WaveFX spinning disc  
187 confocal system (Quorum Technologies, Guelph, Ontario) with 491 nm and 561 nm solid  
188 state laser lines for excitation of green and red (Alexa-488 and Alexa-594), combined with  
189 appropriate BrightLine single-bandpass emission filters (536/40 nm and 624/40 nm,  
190 Semrock). For DAPI visualization, wide-field z-series were acquired at the same time with a  
191 DAPI fluorescence filter cube (Chroma Technology). The CCD camera used to capture the  
192 images was a Hamamatsu ImagEM C-9100.

193

194 **Western blotting:** Myotubes or skeletal muscles were homogenized in a lysis buffer  
195 containing 10 µl of protease inhibitor cocktail (Sigma-Aldrich). Protein homogenates were  
196 electrophoretically separated on SDS-polyacrylamide gels and transferred to polyvinylidene  
197 difluoride membranes (PVDF; Bio-Rad), blocked in 5% skim milk and incubated overnight  
198 at 4°C. The following primary antibodies (all from Santa Cruz Biotechnology) were used:  
199 anti-SERCA-1a, anti-SERCA-2a, anti-Stim1, anti-calsequestrin, and anti-RANK anti-

200 GAPDH. The membranes were washed and incubated with appropriate HRP-conjugated  
201 secondary antibodies (Santa Cruz Biotechnology). Protein bands were revealed using the  
202 ECL-Plus chemiluminescent detection system (Perkin-Elmer). Films (Denville scientific inc.)  
203 were used to detect a chemiluminescent signal, scanned, and analyzed using Quantity One  
204 software (v4.6.6, Bio-Rad) (10).

205 **Calcium measurements:** In another set of experiments, the concentration of total  $\text{Ca}^{2+}$  in Sol  
206 and EDL muscles was determined using the  $\text{Ca}^{2+}$ -dependent UV absorbance of 1,2-Bis (2-  
207 Aminophenoxy) ethane-*N,N,N',N'*-tetraacetic acid (BAPTA) which is a good estimate of  
208  $[\text{CaT}]$  in the SR (30). Briefly, whole Sol and EDL muscles from 12 week-old mice were  
209 weighed and homogenized in a solution containing 0.3 mM BAPTA and sodium dodecyl  
210 sulphate (SDS) detergent to dissolve the surface and SR membranes. The mixture was then  
211 centrifuged removing proteins and other insoluble muscle components to prevent unwanted  
212 absorbance or light scattering. To determine the amount of total  $\text{Ca}^{2+}$ , the supernatant was  
213 divided into four aliquots for separate absorbance measurements taken at 292 nm: 1) the  
214 supernatant alone; 2) The UV absorbance spectrum (240-390 nm) of the supernatant plus 1  
215 mM EGTA added to give a zero  $\text{Ca}^{2+}$  BAPTA spectrum; 3) the supernatant with a known  
216 amount of  $\text{Ca}^{2+}$  standard added; and 4) the supernatant with excess  $\text{Ca}^{2+}$  added to complex  
217 essentially all of the binding sites on BAPTA with  $\text{Ca}^{2+}$ . From the absorbance data and the  
218 equations given by Lamboley et al. (30), values of total  $\text{Ca}^{2+}$  concentration were estimated  
219 and reported here in units of mmoles/kg muscle weight.  $[\text{CaT}]$  measurements include the  
220 following components: extracellular ( $[\text{CaT}]_{\text{EC}}$ ), intracellular outside of the SR ( $[\text{CaT}]_{\text{NonSR}}$ ),  
221 and intracellular inside the SR ( $[\text{CaT}]_{\text{SR}}$ ). The  $\text{Ca}^{2+}$  chelator, BAPTA, should provide the best  
222 estimate of  $[\text{CaT}]_{\text{SR}}$  under physiological conditions (30).

223

224 **SERCA parameters:** Homogenates from the muscles of WT and KO mice were used to

225 determine  $\text{Ca}^{2+}$  dependent  $\text{Ca}^{2+}$ -ATPase activity using a spectrophotometric assay  
226 (SPECTRAMax Plus; Molecular Devices) (47). Briefly, reaction buffer (200 mM KCl, 20  
227 mM HEPES (pH 7.0), 15 mM  $\text{MgCl}_2$ , 1 mM EGTA, 10 mM  $\text{NaN}_3$ , 5 mM ATP and 10 mM  
228 PEP) containing 18 U/mL of both LDH and PK, as well as the homogenate were added to test  
229 tubes containing 15 different concentrations of  $\text{Ca}^{2+}$ , ranging between 7.6 and 4.7 pCa units  
230 in the presence and absence of ionophore A23187 (4.2  $\mu\text{M}$ ). In the absence of the ionophore,  
231  $\text{Ca}^{2+}$  accumulates inside the SR vesicle and causes back-inhibition of SERCA pumps, which  
232 is more relevant to the physiological system found in skeletal muscle. Aliquots (100  $\mu\text{l}$ ) were  
233 then transferred in duplicate to a clear bottom 96-well plate (Costar, Corning Incorporated,  
234 NY), where 0.3 mM NADH was added to start the reaction. The plate was read at a  
235 wavelength of 340 nm for 30 min at 37°C. The different concentrations of  $\text{Ca}^{2+}$  in the wells  
236 were used to determine the maximal enzyme activity ( $V_{\text{max}}$ ) and pCa50, which is defined as  
237 the  $[\text{Ca}^{2+}]_f$  required to achieve 50% of  $V_{\text{max}}$ . Lastly, cyclopiazonic acid (CPA; 40  $\mu\text{M}$ ), a  
238 highly specific SERCA inhibitor, was used to determine background activity which was  
239 subtracted from the total  $\text{Ca}^{2+}$ -ATPase activity measured in muscle homogenate. All data  
240 were then plotted against the negative logarithm of  $[\text{Ca}^{2+}]_f$  (pCa) using basic statistical  
241 software (GraphPad Prism™ version 4) to determine  $V_{\text{max}}$  and pCa50. pCa50 was  
242 determined by non-linear regression curve fitting using the sigmoidal dose response.

243

244 **Statistical analyses.** All values are expressed as means  $\pm$  SEM. The data were analyzed with  
245 Student's t-test, Chi-square test or one-way ANOVA followed by a Tukey's test (InStat). The  
246 levels of significance were set at \*  $p < 0.05$ , \*\*  $p < 0.01$ , \*\*\*  $p < 0.001$  for genotype ( $\text{RANK}^{f/f}$  vs  
247  $\text{RANK}^{\text{mko}}$ ) or #  $p < 0.05$  for treatment (Sham vs Den).

248

249

250

251 **Results**

252 ***RANK is expressed in fully differentiated C2C12 myotubes and at the sarcolemmal***  
253 ***membrane of skeletal muscle***

254 To assess RANK expression in muscle cells, we first analysed its expression in C2C12  
255 myoblasts and differentiated myotubes. RANK was found to be expressed in C2C12  
256 myotubes but not in proliferating C2C12 myoblasts (Fig. 1a). We next analysed RANK  
257 expression in skeletal muscle cells *in situ* using confocal microscopy. Confocal  
258 immunofluorescence confirmed the presence of RANK protein on the membrane of fast-  
259 twitch (EDL) (Fig. 1b) and slow-twitch (Sol; data not shown) skeletal muscle fibers. To  
260 confirm specific RANK expression in muscle, we crossed *RANK<sup>ff</sup>* mice onto a muscle  
261 creatine kinase-Cre background to generate muscle-specific RANK knockout mice (*RANK<sup>mko</sup>*  
262 mice). PCR results validated the deletion of the RANK allele specifically in skeletal muscle  
263 tissue and partially in heart (Fig. 1c). Deletion efficiency was confirmed at the protein level  
264 in skeletal muscles where RANK immunostaining was not detectable (Fig. 1b).

265

266 ***RANK deletion affects denervated muscle mass and function***

267 To examine the role of RANK/RANKL in muscle pathophysiology, muscle mass,  
268 contractile properties and fiber type proportions were examined in sham and denervated Sol  
269 and EDL muscles from *RANK<sup>ff</sup>* and *RANK<sup>mko</sup>* mice. Denervation and/or RANK deletion did  
270 not influence mouse body weight. Treatment, but not genotype, reduced EDL and Sol muscle  
271 masses when normalized to body weights (Table 1). Intriguingly, denervated EDL muscles  
272 from *RANK<sup>mko</sup>* mice exhibited inotropic effects as determined by the decrease in muscle mass  
273 (Fig. 2a), combined with the partial preservation of maximum specific force ( $sP_0$ ; N/cm<sup>2</sup>)  
274 compared to denervated *RANK<sup>ff</sup>* muscles (Fig. 2b). The absolute force production ( $P_0$ ; g) was  
275 not different between *RANK<sup>ff</sup>* and *RANK<sup>mko</sup>* EDL muscle but RANK deletion prevented the

276 loss of twitch tension ( $P_t$ ) in denervated EDL muscles (Table 2). The contractile properties of  
277 control mice were similar between both genotypes (Table 2). Lastly, the  $P_t/P_0$  ratio was  
278 increased in both Sol and EDL muscles of denervated  $RANK^{mko}$  mice (Fig. 2c), suggesting a  
279 change in myofilament  $Ca^{2+}$  sensitivity and/or SR  $Ca^{2+}$  release.

280

281 Denervation led to decreased fatigue resistance in both Sol and EDL muscles during a  
282 repetitive and glycolytic fatigue protocol (Fig. 2d,e). Both sham and denervated  $RANK^{mko}$   
283 EDL muscles exhibited increased fatigability compared to sham and denervated  $RANK^{ff}$   
284 muscles (Fig. 2d,e). In accordance with the higher fatigability, immunohistochemical fiber  
285 typing showed that the slow-twitch fibers were nearly absent in sham  $RANK^{mko}$  EDL muscles  
286 while the proportion of fast-twitch fibers (IIA+IIX+IIB) was significantly increased in  
287 denervated  $RANK^{mko}$  EDL muscles compared to denervated  $RANK^{ff}$  EDL muscles (Fig. 2f).  
288 The proportion of fiber type over 100% in denervated  $RANK^{mko}$  EDL muscles indicated the  
289 presence of hybrid fibers expressing multiple isoforms of MyHC. No changes in muscle fiber  
290 type were observed in Sol muscles (Fig. 3a) indicating that the impact of muscle RANK  
291 deletion on muscle fatigue and phenotype is limited to fast-twitch EDL muscles. Noticeably,  
292 the proportion of fast-twitch fibers expressing SERCA-1a was reduced and the proportion of  
293 fast-twitch fibers expressing SERCA-2a was increased in  $RANK^{mko}$  Sol and EDL muscles  
294 (Fig 3b).

295

#### 296 ***Total calcium and SERCA activity and expression in $RANK^{ff}$ and $RANK^{mko}$ muscles***

297 Our recent published data show an inverse relationship between [CaT] and muscle mass,  
298 where the highest values of [CaT] are seen with the lowest muscle weights (30). Since  
299 RANK deletion promotes muscle atrophy and prevents force deficits in denervated muscles,  
300 we next measured [CaT] in EDL muscles (Fig. 4a-c). Despite similar muscle masses, the

301 average values of [CaT] were 42% lower in sham *RANK<sup>mko</sup>* relative to sham *RANK<sup>ff</sup>* EDL  
302 muscles (Fig. 4c), indicating that under non pathological conditions muscle RANK is  
303 important in Ca<sup>2+</sup> storage of skeletal muscles. Consistent with the observed inverted  
304 relationship between [CaT] and muscle weights, we found that muscle weights below <4.5  
305 mg had much greater [CaT] than the bigger muscles, but data were non-linear due to a floor  
306 effect in the assay (Fig. 4b). Consistent with the reduced muscle mass in denervated *RANK<sup>mko</sup>*  
307 EDL muscles (Fig. 2a), [CaT] increased by 93% in denervated *RANK<sup>mko</sup>* EDL muscles while  
308 it did not significantly increase in denervated *RANK<sup>ff</sup>* EDL muscles (Fig. 4c).

309

310 Since SERCA is critical for Ca<sup>2+</sup> cycling in the SR, we analyzed SERCA1a and SERCA2a  
311 expression and SERCA activity in Sol and EDL muscle extracts. Western blotting analyses  
312 show that SERCA1a content is significantly reduced in denervated muscles while SERCA2a  
313 content is significantly increased following denervation, independently of the genotype (Fig  
314 4d). No difference in calsequestrin content, a calcium binding protein located in SR, was  
315 observed between *RANK<sup>ff</sup>* and *RANK<sup>mko</sup>* muscles (Fig 4d). However, the content of the  
316 stromal interaction molecule 1 (Stim1), which functions as a calcium sensor in the SR,  
317 increased by 77% and 411% in denervated *RANK<sup>ff</sup>* and *RANK<sup>mko</sup>* EDL muscles, relative to  
318 their respective sham (Fig 4d). The concentration of Stim1 increased significantly by 184%  
319 in denervated *RANK<sup>mko</sup>* compared to denervated *RANK<sup>mko</sup>* EDL muscles. Next, we assessed  
320 SERCA Ca<sup>2+</sup>-dependent ATPase activity in muscle homogenates from sham and denervated  
321 *RANK<sup>ff</sup>* and *RANK<sup>mko</sup>* Sol and EDL muscles over Ca<sup>2+</sup> concentrations ranging from pCa 7.0  
322 to pCa 4.5. Interestingly, upon denervation, maximal SERCA activity was reduced in both  
323 the Sol and EDL muscles (Fig. 4e-g and Fig. 5). Moreover, maximal SERCA activity was  
324 significantly reduced in both the sham and denervated *RANK<sup>mko</sup>* EDL compared to the sham  
325 and denervated *RANK<sup>ff</sup>* EDL (Fig. 4c-f). This inhibitory effect of RANK deletion on SERCA

326 activity was limited to EDL muscles and did not affect Sol muscles. Overall, these findings  
327 demonstrate a direct role for muscle RANK in the regulation of SERCA activity and Stim1  
328 content in fast-twitch EDL muscles.

329

330

331

332 **Discussion**

333 We previously demonstrated that systemic injection of OPG, the decoy receptor of  
334 RANKL, restores muscle force and improves muscle histology in dystrophic *mdx* mice (9).  
335 However, whether the RANK/RANKL/OPG system directly or indirectly affects skeletal  
336 muscle was unknown. In this paper, using muscle specific RANK mutant mice, we  
337 demonstrate that RANK is expressed in skeletal muscle cells where it directly regulates  
338 muscle function. Importantly, muscle-specific RANK deletion protects from denervation-  
339 induced loss of muscle force and modulates total  $\text{Ca}^{2+}$  storage and SERCA activity.

340

341 RANK is well characterized in osteoclasts where it leads to the activation of different  
342 signalling pathways, especially NF- $\kappa$ B and calcium-dependent pathways (5). In skeletal  
343 muscle,  $\text{Ca}^{2+}$  is a master regulator of multiple intracellular processes such as myosin-actin  
344 cross-bridging, protein synthesis and degradation, mitochondrial adaptation and fiber type  
345 shifting, through the control of  $\text{Ca}^{2+}$  sensitive proteases and transcriptional factors such as  
346 NFATc1 (2). Consistent with a role of RANK in the regulation of calcium handling,  
347 conditional deletion of *RANK* in skeletal muscle affected muscle contraction post-  
348 denervation, atrophy and fiber type, all of which are regulated by  $\text{Ca}^{2+}$  (2). Intriguingly,  
349 muscle-specific *RANK* deletion prevents the loss of specific force production but not the loss  
350 of muscle mass following denervation. Without significant changes in muscle mass, muscle  
351 strength can be altered by (1) the amplitude or duration of the  $\text{Ca}^{2+}$  transient or (2) the  
352 sensitivity of the myofilaments to  $\text{Ca}^{2+}$ . For instance, reduced force production in aged  
353 muscle is partially caused by reduced  $\text{Ca}^{2+}$  content and myofilament sensitivity (31). Our  
354 findings show that *RANK*<sup>*mdx*</sup> denervated muscles have higher [CaT], which originates from  
355 increased intracellular calcium stocks (30, 33). Therefore, higher  $\text{Ca}^{2+}$  content potentially  
356 results in greater rates of  $\text{Ca}^{2+}$  release, increased myoplasmic  $\text{Ca}^{2+}$  transients, and, ultimately,



357 preserved muscle force production. These results are supported by the increased specific  
358 force and Pt/P<sub>0</sub> ratio in denervated *RANK*<sup>mk0</sup> EDL muscle, indicating that these muscles are  
359 able to generate a stronger contraction following submaximal stimulation.

360

361 The higher releasable Ca<sup>2+</sup> content is not explained by greater SERCA activity since we  
362 found that denervated *RANK*<sup>mk0</sup> muscles had low SERCA activity rate compared to the  
363 denervated *RANK*<sup>ff</sup>. Moreover, we observed no change in CSQ content making it unlikely to  
364 explain the greater releasable Ca<sup>2+</sup> content; however, in the normal EDL muscles it was  
365 shown that the resting SR Ca<sup>2+</sup> content is only a relatively small proportion of its maximal  
366 content and that Ca<sup>2+</sup> bound to CSQ is only one-third of its saturated level (14, 35, 52). Thus,  
367 it is likely that the increase in [CaT] observed in the denervated *RANK*<sup>mk0</sup> EDL reflects an  
368 increased binding of Ca<sup>2+</sup> in the SR thereby increasing releasable SR Ca<sup>2+</sup> and ultimately  
369 specific force production. In this respect, the relatively greater inhibition of SERCA activity  
370 may serve to prolong the Ca<sup>2+</sup> transient and increase force production, while decreasing the  
371 fatigue resistance. Accordingly, we observed higher muscle strength following a single  
372 contraction (Pt) in denervated *RANK*<sup>mk0</sup> EDL muscle combined with increased fatigability  
373 following repeated maximal contractions. The exact mechanisms lowering SERCA activity in  
374 response to RANK deletion are unknown and require further investigation – and analysis of  
375 sarcolipin and phospholamban, two well-known regulators of the SERCA pump (15),  
376 indicate increased expression of both proteins in response to denervation, however no  
377 significant differences were found between genotype (data not shown).

378

379 Enhanced Ca<sup>2+</sup> entry could be responsible for any increase in SR Ca<sup>2+</sup> content in muscle.  
380 In osteoclasts, RANKL-mediated Ca<sup>2+</sup> entry could arise from intracellular or extracellular  
381 origin (6, 25). Members of the transient receptor potential vanilloid channels (TRPV) family,

382 TRPV2 and TRPV5, were demonstrated to mediate RANKL-induced calcium entry (6, 23).  
383 Store-operated calcium entry (SOCE) channels, that sense declining  $\text{Ca}^{2+}$  ion concentration in  
384 the SR, were also associated with RANKL-induced calcium entry (23). For instance,  
385 silencing of the SOCE channel Orai1 with specific shRNA inhibits RANKL-induced  
386 osteoclastogenesis by suppressing NFATc1 induction (20). Mice lacking SOCE specifically  
387 in skeletal muscle exhibit reduced muscle mass and increased susceptibility to fatigue  
388 whereas *Stim1*<sup>-/-</sup> myotubes failed to refill their stores and altered expression of key SR  
389 proteins (48). Furthermore, the use of SERCA inhibitor suggests that under some conditions  
390 the role of SERCA in replenishing  $\text{Ca}^{2+}$  stores is limited (37). Our current findings that  
391 denervation treatment and RANK deletion markedly increased *Stim1* content (184%) may  
392 explain, in part, the discrepancy between the rise in [CaT] and the depression of SERCA  
393 activity in denervated *RANK*<sup>mk0</sup> EDL muscles. It is thus tempting to speculate that SOCE  
394 would compensate for the lack of SERCA activity in denervated *RANK*<sup>mk0</sup> EDL muscles.  
395 The mechanisms by which RANKL/RANK controls  $\text{Ca}^{2+}$  storage in skeletal muscle cells  
396 requires further experiments, nevertheless our findings provide the first evidence that RANK  
397 is a novel regulator of  $\text{Ca}^{2+}$  storage in skeletal muscle cells.

398

399 With respect to EDL muscle fatigability, we found that both denervation and RANK  
400 deletion led to higher fatigability than their wild type and sham-operated counterparts.  
401 Consistent with this observation, we found that *RANK*<sup>mk0</sup> muscles increased the number of  
402 fast-twitch type II fibers; however, the disproportionate increase of fatigability in *RANK*<sup>mk0</sup>  
403 muscle compared to the relatively modest changes in fiber type and that no changes on  
404 muscle contractility, fatigue and phenotype were observed in Sol muscles, suggests that the  
405 muscle fiber type phenotype may not be the main reason to explain the fatigue in *RANK*<sup>mk0</sup>  
406 muscle. Indeed, the decreased fatigue resistance observed following denervation was

407 associated with an increased proportion of type I fibres in both *RANK<sup>fl/fl</sup>* and *RANK<sup>mk0</sup>* Sol and  
408 EDL muscles. It could be speculated that the altered calcium signalling following muscle-  
409 specific *RANK* deletion impairs mitochondrial function given the well-established role of the  
410 calcium-dependent effectors calcineurin and NFATc1 in enhancing muscle endurance and  
411 mitochondrial respiratory capacity (21). Nevertheless, our findings indicate that *RANK*  
412 deletion enhances force production, promotes a fast-twitch phenotype and fatigability while  
413 increasing stim1 content and decreasing SERCA activity.

414

#### 415 *Perspective and conclusion*

416 Osteoporosis and muscle wasting occur simultaneously in a variety of pathologies,  
417 although common signalling pathways between these two processes were not identified (Fig.  
418 6). Here, we show that in addition to its role in bone homeostasis, *RANK* signalling also  
419 regulates Ca<sup>2+</sup> storage, muscle mass, and muscle performance. Muscle-specific deletion of  
420 *RANK* has an inotropic effect on denervated fast-twitch EDL muscles, largely composed of  
421 type IIA, IIX, and IIB fibers. Fast-twitch fibers are usually the first to be affected in several  
422 forms of muscular and neuromuscular diseases and aging conditions, leading to premature  
423 loss of function and important incapacities (8). Our findings show for the first time that fast-  
424 twitch fibers may be specifically targeted to enhance their force production. Although these  
425 results are preliminary and the long-term effects remain to be determined, this discovery  
426 opens a whole new field of research and new therapeutics avenues for conditions affecting in  
427 synchrony bone and skeletal muscle and potentially heart diseases.

428

429 Disclosures section: J.F., S.S.D., N.A.D., and J.M.P. conceived the project and its design;  
430 S.S.D., N.A.D., P.B., A.B.P, V.A.F., D.G., S.A.K.G., O.D., R.T., P.C.P. and E.L. performed  
431 experiments and data analysis; J.F., S.S.D., and N.A.D. wrote the manuscript; and all authors  
432 checked for scientific content and approved the final manuscript. JF is supported by CIHR  
433 and NSERC and JMP by an advanced ERC grant and the Austrian academy of Sciences. The  
434 authors declare no competing interests.

435

436

437

438

- 439 1. **Allen DG, Gervasio OL, Yeung EW, Whitehead NP.** Calcium and the damage  
440 pathways in muscular dystrophy. *Can J Physiol Pharmacol* 88: 83–91, 2010.
- 441 2. **Berchtold MW, Brinkmeier H, Müntener M.** Calcium ion in skeletal muscle: its  
442 crucial role for muscle function, plasticity, and disease. *Physiol Rev* 80: 1215–1265,  
443 2000.
- 444 3. **Bloomfield SA.** Changes in musculoskeletal structure and function with  
445 prolonged bed rest. *Med Sci Sports Exerc* 29: 197–206, 1997.
- 446 4. **Boss GR, Seegmiller JE.** Age-related physiological changes and their clinical  
447 significance. *West J Med* 135: 434–440, 1981.
- 448 5. **Boyle WJ, Simonet WS, Lacey DL.** Osteoclast differentiation and activation.  
449 *Nature* 423: 337–342, 2003.
- 450 6. **Chamoux E, Bisson M, Payet MD, Roux S.** TRPV-5 mediates a receptor activator  
451 of NF-kappaB (RANK) ligand-induced increase in cytosolic Ca<sup>2+</sup> in human osteoclasts  
452 and down-regulates bone resorption. *J Biol Chem* 285: 25354–25362, 2010.
- 453 7. **Chin ER.** Role of Ca<sup>2+</sup>/calmodulin-dependent kinases in skeletal muscle  
454 plasticity. *J Appl Physiol Bethesda Md* 1985 99: 414–423, 2005.
- 455 8. **Ciciliot S, Rossi AC, Dyar KA, Blaauw B, Schiaffino S.** Muscle type and fiber  
456 type specificity in muscle wasting. *Int J Biochem Cell Biol* 45: 2191–2199, 2013.
- 457 9. **Dufresne SS, Dumont NA, Bouchard P, Lavergne É, Penninger JM, Frenette J.**  
458 Osteoprotegerin Protects against Muscular Dystrophy. *Am J Pathol* 185: 920–926, 2015.
- 459 10. **Dufresne SS, Frenette J.** Investigation of wild-type and mycolactone-negative  
460 mutant *Mycobacterium ulcerans* on skeletal muscle: IGF-1 protects against  
461 mycolactone-induced muscle catabolism. *Am J Physiol Regul Integr Comp Physiol* 304:  
462 R753–762, 2013.
- 463 11. **Dumont N, Frenette J.** Macrophages protect against muscle atrophy and  
464 promote muscle recovery in vivo and in vitro: a mechanism partly dependent on the  
465 insulin-like growth factor-1 signaling molecule. *Am J Pathol* 176: 2228–2235, 2010.
- 466 12. **Francini F, Formigli L, Meacci E, Vassalli M, Nosi D, Quercioli F, Tiribilli B,**  
467 **Bencini C, Squecco R, Bruni P, Orlandini SZ.** Ca<sup>2+</sup> homeostasis and cytoskeletal  
468 rearrangement operated by sphingosine 1-phosphate in C2C12 myoblastic cells. *J*  
469 *Gravitational Physiol J Int Soc Gravitational Physiol* 9: P281–282, 2002.
- 470 13. **Frenette J, St-Pierre M, Côté CH, Mylona E, Pizza FX.** Muscle impairment  
471 occurs rapidly and precedes inflammatory cell accumulation after mechanical loading.  
472 *Am J Physiol Regul Integr Comp Physiol* 282: R351–357, 2002.
- 473 14. **Fryer MW, Stephenson DG.** Total and sarcoplasmic reticulum calcium contents  
474 of skinned fibres from rat skeletal muscle. *J Physiol* 493 ( Pt 2): 357–370, 1996.
- 475 15. **Gamu D, Bombardier E, Smith IC, Fajardo VA, Tupling AR.** Sarcolipin provides  
476 a novel muscle-based mechanism for adaptive thermogenesis. *Exerc Sport Sci Rev* 42:  
477 136–142, 2014.
- 478 16. **Goldspink DF.** The effects of denervation on protein turnover of the soleus and  
479 extensor digitorum longus muscles of adult mice. *Comp Biochem Physiol B* 61: 37–41,  
480 1978.
- 481 17. **Hanada R, Hanada T, Sigl V, Schramek D, Penninger JM.** RANKL/RANK-  
482 beyond bones. *J Mol Med Berl Ger* 89: 647–656, 2011.
- 483 18. **Hanada R, Leibbrandt A, Hanada T, Kitaoka S, Furuyashiki T, Fujihara H,**  
484 **Trichereau J, Paolino M, Qadri F, Plehm R, Klaere S, Komnenovic V, Mimata H,**  
485 **Yoshimatsu H, Takahashi N, von Haeseler A, Bader M, Kilic SS, Ueta Y, Pifl C,**  
486 **Narumiya S, Penninger JM.** Central control of fever and female body temperature by  
487 RANKL/RANK. *Nature* 462: 505–509, 2009.

- 488 19. **Hindi SM, Sato S, Choi Y, Kumar A.** Distinct roles of TRAF6 at early and late  
489 stages of muscle pathology in the mdx model of Duchenne muscular dystrophy. *Hum*  
490 *Mol Genet* 23: 1492–1505, 2014.
- 491 20. **Hwang S-Y, Putney JW.** Orai1-mediated calcium entry plays a critical role in  
492 osteoclast differentiation and function by regulating activation of the transcription  
493 factor NFATc1. *FASEB J Off Publ Fed Am Soc Exp Biol* 26: 1484–1492, 2012.
- 494 21. **Jiang LQ, Garcia-Roves PM, de Castro Barbosa T, Zierath JR.** Constitutively  
495 active calcineurin in skeletal muscle increases endurance performance and  
496 mitochondrial respiratory capacity. *Am J Physiol Endocrinol Metab* 298: E8–E16, 2010.
- 497 22. **Jost PD.** Simulating human space physiology with bed rest. *Hippokratia* 12 Suppl  
498 1: 37–40, 2008.
- 499 23. **Kajiya H, Okamoto F, Nemoto T, Kimachi K, Toh-Goto K, Nakayana S, Okabe**  
500 **K.** RANKL-induced TRPV2 expression regulates osteoclastogenesis via calcium  
501 oscillations. *Cell Calcium* 48: 260–269, 2010.
- 502 24. **Kohn AD, Moon RT.** Wnt and calcium signaling:  $\beta$ -Catenin-independent  
503 pathways. *Cell Calcium* 38: 439–446, 2005.
- 504 25. **Komarova SV, Pilkington MF, Weidema AF, Dixon SJ, Sims SM.** RANK ligand-  
505 induced elevation of cytosolic  $Ca^{2+}$  accelerates nuclear translocation of nuclear factor  
506 kappa B in osteoclasts. *J Biol Chem* 278: 8286–8293, 2003.
- 507 26. **Kong YY, Feige U, Sarosi I, Bolon B, Tafuri A, Morony S, Capparelli C, Li J,**  
508 **Elliott R, McCabe S, Wong T, Campagnuolo G, Moran E, Bogoch ER, Van G, Nguyen**  
509 **LT, Ohashi PS, Lacey DL, Fish E, Boyle WJ, Penninger JM.** Activated T cells regulate  
510 bone loss and joint destruction in adjuvant arthritis through osteoprotegerin ligand.  
511 *Nature* 402: 304–309, 1999.
- 512 27. **Kramer I, Halleux C, Keller H, Pegurri M, Gooi JH, Weber PB, Feng JQ,**  
513 **Bonewald LF, Kneissel M.** Osteocyte Wnt/beta-catenin signaling is required for normal  
514 bone homeostasis. *Mol Cell Biol* 30: 3071–3085, 2010.
- 515 28. **Kumar A, Bhatnagar S, Paul PK.** TWEAK and TRAF6 regulate skeletal muscle  
516 atrophy. *Curr Opin Clin Nutr Metab Care* 15: 233–239, 2012.
- 517 29. **Lacey D., Timms E, Tan H-L, Kelley M., Dunstan C., Burgess T, Elliott R,**  
518 **Colombero A, Elliott G, Scully S, Hsu H, Sullivan J, Hawkins N, Davy E, Capparelli C,**  
519 **Eli A, Qian Y-X, Kaufman S, Sarosi I, Shalhoub V, Senaldi G, Guo J, Delaney J, Boyle**  
520 **W.** Osteoprotegerin Ligand Is a Cytokine that Regulates Osteoclast Differentiation and  
521 Activation. *Cell* 93: 165–176, 1998.
- 522 30. **Lambley CRH, Kake Guena SA, Touré F, Hébert C, Yaddaden L, Nadeau S,**  
523 **Bouchard P, Wei-LaPierre L, Lainé J, Rousseau EC, Frenette J, Protasi F, Dirksen**  
524 **RT, Pape PC.** New method for determining total calcium content in tissue applied to  
525 skeletal muscle with and without calcequestrin. *J Gen Physiol* 145: 127–153, 2015.
- 526 31. **Lambley CR, Wyckelsma VL, Dutka TL, McKenna MJ, Murphy RM, Lamb GD.**  
527 Contractile properties and sarcoplasmic reticulum calcium content in type I and type II  
528 skeletal muscle fibres in active aged humans. *J Physiol* 593: 2499–2514, 2015.
- 529 32. **Leibbrandt A, Penninger JM.** RANK/RANKL: regulators of immune responses  
530 and bone physiology. *Ann N Y Acad Sci* 1143: 123–150, 2008.
- 531 33. **Manno C, Ríos E.** A better method to measure total calcium in biological samples  
532 yields immediate payoffs. *J Gen Physiol* 145: 167–171, 2015.
- 533 34. **Melzer W, Herrmann-Frank A, Lüttgau HC.** The role of  $Ca^{2+}$  ions in excitation-  
534 contraction coupling of skeletal muscle fibres. *Biochim Biophys Acta* 1241: 59–116,  
535 1995.
- 536 35. **Murphy RM, Larkins NT, Mollica JP, Beard NA, Lamb GD.** Calcequestrin

537 content and SERCA determine normal and maximal Ca<sup>2+</sup> storage levels in sarcoplasmic  
538 reticulum of fast- and slow-twitch fibres of rat. *J Physiol* 587: 443–460, 2009.

539 36. **Nagy V, Penninger JM.** The RANKL-RANK Story. *Gerontology* ( February 14,  
540 2015). doi: 10.1159/000371845.

541 37. **Okubo Y, Suzuki J, Kanemaru K, Nakamura N, Shibata T, Iino M.** Visualization  
542 of Ca<sup>2+</sup> Filling Mechanisms upon Synaptic Inputs in the Endoplasmic Reticulum of  
543 Cerebellar Purkinje Cells. *J Neurosci* 35: 15837–15846, 2015.

544 38. **Page G, Miossec P.** RANK and RANKL expression as markers of dendritic cell-T  
545 cell interactions in paired samples of rheumatoid synovium and lymph nodes. *Arthritis*  
546 *Rheum* 52: 2307–2312, 2005.

547 39. **Pang MYC, Eng JJ, McKay HA, Dawson AS.** Reduced hip bone mineral density is  
548 related to physical fitness and leg lean mass in ambulatory individuals with chronic  
549 stroke. *Osteoporos Int J Establ Result Coop Eur Found Osteoporos Natl Osteoporos Found*  
550 *USA* 16: 1769–1779, 2005.

551 40. **Patterson MF.** Denervation produces different single fiber phenotypes in fast-  
552 and slow-twitch hindlimb muscles of the rat. *AJP Cell Physiol* 291: 518–528, 2006.

553 41. **Perlot T, Penninger JM.** Development and function of murine B cells lacking  
554 RANK. *J Immunol Baltim Md* 1950 188: 1201–1205, 2012.

555 42. **Sandri M.** Apoptotic signaling in skeletal muscle fibers during atrophy. *Curr Opin*  
556 *Clin Nutr Metab Care* 5: 249–253, 2002.

557 43. **Schiaffino S, Gorza L, Sartore S, Saggin L, Ausoni S, Vianello M, Gundersen K,**  
558 **Lømo T.** Three myosin heavy chain isoforms in type 2 skeletal muscle fibres. *J Muscle*  
559 *Res Cell Motil* 10: 197–205, 1989.

560 44. **Segal SS, Faulkner JA.** Temperature-dependent physiological stability of rat  
561 skeletal muscle in vitro. *Am J Physiol* 248: C265–270, 1985.

562 45. **Sigl V, Penninger JM.** RANKL/RANK - from bone physiology to breast cancer.  
563 *Cytokine Growth Factor Rev* 25: 205–214, 2014.

564 46. **Simonet W., Lacey D., Dunstan C., Kelley M, Chang M-S, Lüthy R, Nguyen H.,**  
565 **Wooden S, Bennett L, Boone T, Shimamoto G, DeRose M, Elliott R, Colombero A,**  
566 **Tan H-L, Trail G, Sullivan J, Davy E, Bucay N, Renshaw-Gegg L, Hughes T., Hill D,**  
567 **Pattison W, Campbell P, Sander S, Van G, Tarpley J, Derby P, Lee R, Boyle W.**  
568 Osteoprotegerin: A Novel Secreted Protein Involved in the Regulation of Bone Density.  
569 *Cell* 89: 309–319, 1997.

570 47. **Smith IC, Bombardier E, Vigna C, Tupling AR.** ATP consumption by  
571 sarcoplasmic reticulum Ca<sup>2+</sup> pumps accounts for 40-50% of resting metabolic rate in  
572 mouse fast and slow twitch skeletal muscle. *PloS One* 8: e68924, 2013.

573 48. **Stiber J, Hawkins A, Zhang Z-S, Wang S, Burch J, Graham V, Ward CC, Seth M,**  
574 **Finch E, Malouf N, Williams RS, Eu JP, Rosenberg P.** STIM1 signalling controls store-  
575 operated calcium entry required for development and contractile function in skeletal  
576 muscle. *Nat Cell Biol* 10: 688–697, 2008.

577 49. **Sun H, Gong Y, Qiu J, Chen Y, Ding F, Zhao Q.** TRAF6 Inhibition Rescues  
578 Dexamethasone-Induced Muscle Atrophy. *Int J Mol Sci* 15: 11126–11141, 2014.

579 50. **Sun H, Qiu J, Chen Y, Yu M, Ding F, Gu X.** Proteomic and bioinformatic analysis  
580 of differentially expressed proteins in denervated skeletal muscle. *Int. J. Mol. Med.* ( April  
581 8, 2014). doi: 10.3892/ijmm.2014.1737.

582 51. **Theill LE, Boyle WJ, Penninger JM.** RANK-L and RANK: T cells, bone loss, and  
583 mammalian evolution. *Annu Rev Immunol* 20: 795–823, 2002.

584 52. **Trinh HH, Lamb GD.** Matching of sarcoplasmic reticulum and contractile  
585 properties in rat fast- and slow-twitch muscle fibres. *Clin Exp Pharmacol Physiol* 33:

586 591–600, 2006.  
587 53. **Walsh MC, Choi Y.** Biology of the RANKL/RANK/OPG System in Immunity,  
588 Bone, and Beyond. *Front Immunol* 5, 2014.  
589 54. **Yang Y-M, Kim MS, Son A, Hong JH, Kim K-H, Seo JT, Lee S-I, Shin DM.**  
590 Alteration of RANKL-Induced Osteoclastogenesis in Primary Cultured Osteoclasts From  
591 SERCA2 +/- Mice. *J Bone Miner Res* 24: 1763–1769, 2009.  
592 55. **Yasuda H, Shima N, Nakagawa N, Yamaguchi K, Kinosaki M, Mochizuki S,**  
593 **Tomoyasu A, Yano K, Goto M, Murakami A, Tsuda E, Morinaga T, Higashio K,**  
594 **Udagawa N, Takahashi N, Suda T.** Osteoclast differentiation factor is a ligand for  
595 osteoprotegerin/osteoclastogenesis-inhibitory factor and is identical to  
596 TRANCE/RANKL. *Proc Natl Acad Sci U S A* 95: 3597–3602, 1998.  
597

598

599

600

601

602

603

604

605

606

607

608

609

610

611

612

613

614

615

616



617

**Table caption**

618 **Table 1: Body weights and muscle mass normalized to body weight of mice.**

619 Denervation and/or muscle RANK deletion did not influence body weight. Treatment, but  
620 not genotype, reduced EDL and Sol muscle mass normalized to body weight. Data are  
621 presented as mean +/- SEM, n=7. The level of significance was set at # p<0.05 for treatment  
622 (Sham vs Den).

623

624 **Table 2: Contractile properties of Sol and EDL muscles.** Ctr, sham and denervated

625 RANK<sup>f/f</sup> and RANK<sup>mk0</sup> SOL and EDL muscles were incubated ex vivo and electrically  
626 stimulated to record maximal absolute force (P<sub>0</sub>) and twitch tension P<sub>t</sub> (g). P<sub>0</sub> (g) decreased  
627 independently of genotype following denervation. However, muscle RANK deletion  
628 prevented the loss of twitch force in denervated EDL muscles. No difference in P<sub>0</sub> and P<sub>t</sub>  
629 were observed in muscle RANK deletion of control mice. Data are presented as mean +/-  
630 SEM, n=7. The level of significance was set at # p<0.05 for treatment (Sham vs Den).

631

632

633

634

635

636

637

638

639

640

641

642

643

644

645

### Figure caption

646 **Figure 1: RANK expression in skeletal muscles and myotubes. (a)** Western blot showing  
647 that fully differentiated C2C12 myotubes but not myoblasts express RANK protein. GAPDH  
648 is shown as a loading control **(b)** Confocal images showing colocalization of intracellular  
649 face of cytoplasmic membrane/sarcolemma dystrophin (green) and RANK (red) in  $RANK^{f/f}$   
650 and the absence of RANK in  $RANK^{mko}$  EDL muscles. Thymus sections were used as positive  
651 controls for RANK immunofluorescence. Omission of primary antibody was used as a  
652 negative control. Because non muscle cells in skeletal muscles can also express RANK,  
653 confocal images, rather than Western blots, were required to confirm the absence of muscle  
654 RANK in  $RANK^{mko}$  mice. Bar =100  $\mu$ m. **(c)** PCR analysis of genomic DNA isolated from  
655 Sol muscle, EDL muscle, heart, liver, spleen and kidney showing efficient Cre-mediated  
656 recombination of loxP sites in skeletal muscles from  $RANK^{mko}$  mice.

657

658 **Figure 2: Impact of RANK deletion on muscle contractility, fatigue and phenotype. (a)**  
659 Muscle atrophy was significantly more pronounced in denervated  $RANK^{mko}$  relative to  
660  $RANK^{f/f}$  EDL muscles. **(b)** However, ex vivo force measurements show that RANK ablation  
661 preserves the specific force tension of denervated (Den) EDL muscles but not in slow-twitch  
662 Sol muscles. **(c)** RANK deletion increases Pt/P<sub>0</sub> ratio in Sol and EDL muscles following  
663 denervation. **(d)** Muscle glycolytic fatigue protocol was induced by a train of stimulations  
664 (200 ms on: 800 ms off, 50 Hz) until Sol muscles force reach 70% of its initial force. Fatigue  
665 time is decreased in denervated muscle but similar between  $RANK^{f/f}$  and  $RANK^{mko}$  muscles.  
666 **(e)** Muscle glycolytic fatigue protocol was induced by a train of stimulations (200 ms on: 800  
667 ms off, 50 Hz) until EDL muscles force reach 50% of its initial force. Sham and denervated  
668  $RANK^{mko}$  EDL muscles exhibit increased fatigability compared to sham and denervated  
669  $RANK^{f/f}$  EDL muscles. **(f)** Fiber typing of EDL muscle analysis showed that the slow-twitch

670 fibers were nearly absent in sham *RANK<sup>mko</sup>* EDL muscles while the proportion of fast-twitch  
671 fibers (IIA+IIB+IIX) was significantly increased in denervated *RANK<sup>mko</sup>* EDL muscles  
672 compared to denervated *RANK<sup>ff</sup>* EDL muscles. The levels of significance were set at \*  
673  $p < 0.05$ , \*\*  $p < 0.01$ , \*\*\*  $p < 0.001$  for genotype (*Rank<sup>ff</sup>* vs *Rank<sup>mko</sup>*) or #  $p < 0.05$  for treatment  
674 (Sham vs Den). Data are presented as mean +/- SEM, n = 3-7.

675

676 **Figure 3: Percentage of type I and II fibers in Sol muscles and proportion of each fiber**  
677 **type expressing SERCA-1a and SERCA-2a in Sol and EDL muscles. (a)** As opposed to  
678 fast-twitch EDL muscles, no changes in phenotype were observed in sham or denervated  
679 *RANK<sup>ff</sup>* and *RANK<sup>mko</sup>* in Sol muscles. **(b)** Sham and denervated *RANK<sup>mko</sup>* muscles  
680 exhibited a lower proportion of fast-twitch fibers expressing SERCA-1a and a higher  
681 proportion of fast-twitch fibers expressing SERCA-2a. The levels of significance were set at  
682 \*  $p < 0.05$ , \*\*  $p < 0.01$ , \*\*\*  $p < 0.001$  for genotype (*Rank<sup>ff</sup>* vs *Rank<sup>mko</sup>*) or #  $p < 0.05$  for  
683 treatment (Sham vs Den). Data are presented as mean +/- SEM, n = 6-8.

684

685 **Figure 4: Total calcium content, SERCA activity and calcium protein contents in**  
686 ***RANK<sup>ff</sup>* and *RANK<sup>mko</sup>* EDL muscles. (a-c)** [CaT] was decreased in sham *RANK<sup>mko</sup>* EDL  
687 muscles relative to sham *RANK<sup>ff</sup>* EDL muscles but increased sharply in denervated  
688 *RANK<sup>mko</sup>* EDL muscles. **(d)** Western blots show that SERCA-1a content is reduced while  
689 SERCA-2a content is increased following denervation. No changes in calsequestrin content  
690 were observed, but Stim1 content increased markedly in denervated *RANK<sup>mko</sup>* EDL muscles.  
691 **(e)** SERCA  $\text{Ca}^{2+}$ -dependent ATPase activity was assessed in muscle homogenates from sham  
692 and denervated *RANK<sup>ff</sup>* and *RANK<sup>mko</sup>* EDL muscles over  $\text{Ca}^{2+}$  concentrations ranging from  
693 pCa 7.4 to pCa 5.0 **(f)** maximal ATPase activity ( $V_{\text{max}}$ ) and **(g)** pCa value required to elicit  
694 50% of maximal activity (pCa50). The levels of significance were set at \*  $p < 0.05$ , \*\*  $p < 0.01$ ,

695 \*\*\*  $p < 0.001$  for genotype (Rank<sup>ff</sup> vs Rank<sup>mko</sup>) or #  $p < 0.05$  for treatment (Sham vs Den).

696 Data are presented as mean +/- SEM, n = 3-7.

697

698 **Figure 5: SERCA Ca<sup>2+</sup>-dependent ATPase parameters from sham and denervated**

699 **RANK<sup>ff</sup> and RANK<sup>mko</sup> in Sol muscles.** Denervation induced a significant reduction of (a)

700 SERCA Ca<sup>2+</sup> dependent ATPase activity and Vmax (b) maximal ATPase activity (Vmax) (c)

701 pCa value required to elicit 50% of maximal activity (pCa50) were similar between control

702 and experimental Sol muscles. The level of significance between genotype (Rank<sup>ff</sup>/Rank<sup>mko</sup>)

703 was set at \*  $p < 0.05$ , \*\*  $p < 0.01$ , \*\*\*  $p < 0.001$  and set at #  $p < 0.05$  between treatment

704 (Sham/Den). Data are presented as mean +/- SEM, n = 3-7.

705

706 **Figure 6: Schematic representation of RANK/RANKL/OPG pathway as common**

707 **regulator of bone and muscle cells.** In osteoclast, RANK/RANKL interaction regulates

708 osteoclastogenesis and/or cell apoptosis through modulation of SERCA activity, Ca<sup>2+</sup>

709 oscillation, Ca<sup>2+</sup>-calcineurin-NFAT and NF- $\kappa$ B pathways. Muscle cells also express RANK

710 and RANK/RANKL interaction is an important regulator of SERCA activity, calcium storage

711 in fast-twitch EDL muscles. These results highlight the importance of a common signalling

712 pathway opening potentially new treatment for both skeletal muscle and bone.

713

714

715

716

**Table 1**

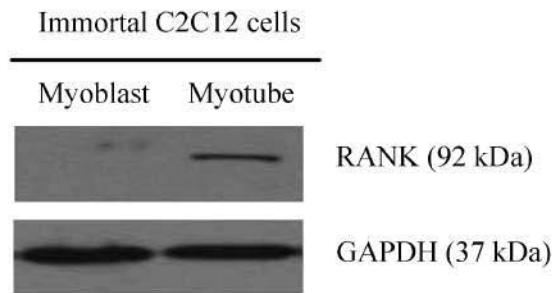
	<b>Mice</b>			
	Sham <sup>f/f</sup>	Den <sup>f/f</sup>	Sham <sup>mko</sup>	Den <sup>mko</sup>
<b>Body weight (g)</b>	24.7 ± 0.8	24.3 ± 0.7	23.8 ± 1.4	24.5 ± 1.9
<b>EDL muscle weight / Body weight</b>	0,34 ± 0,05	0,28 # ± 0,02	0,38 ± 0,04	0,25 # ± 0,04
<b>Sol muscle weight / Body weight</b>	0,29 ± 0,04	0,24 # ± 0,03	0,26 ± 0,03	0,23 # ± 0,04

**Table 2**

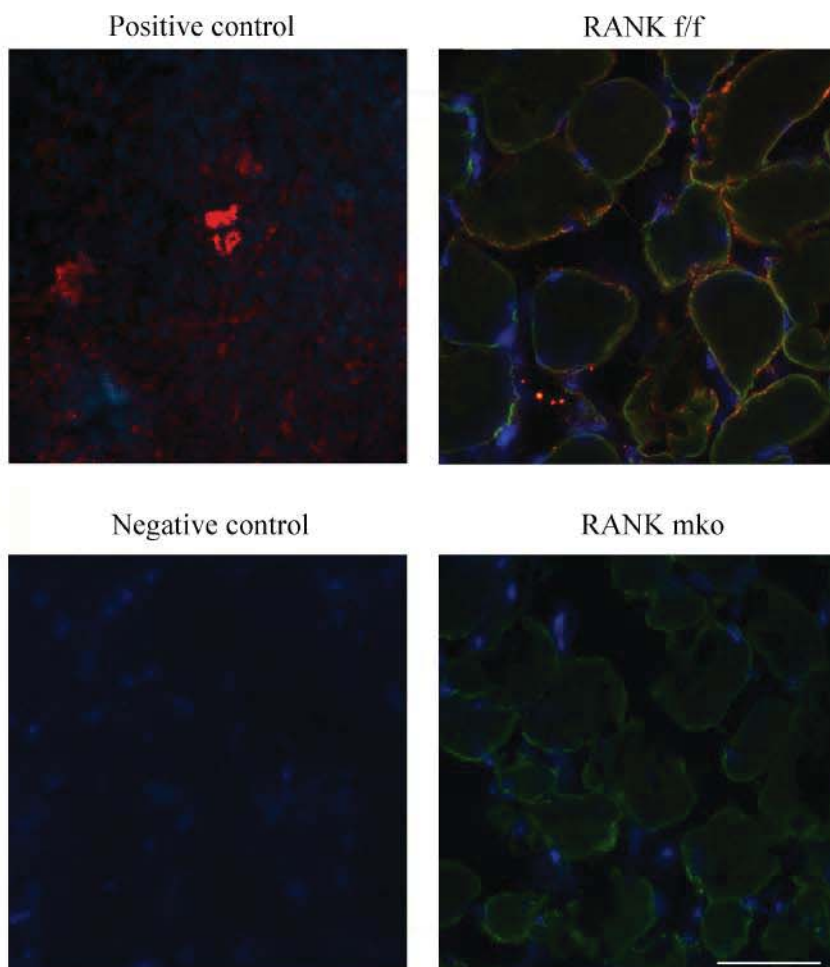
	<b>Sol</b>						<b>EDL</b>					
	Ctr <sup>f/ε</sup>	Sham <sup>ff</sup>	Den <sup>ff</sup>	Ctr <sup>mko</sup>	Sham <sup>mko</sup>	Den <sup>mko</sup>	Ctr <sup>f/ε</sup>	Sham <sup>ff</sup>	Den <sup>ff</sup>	Ctr <sup>mko</sup>	Sham <sup>mko</sup>	Den <sup>mko</sup>
<b>P<sub>0</sub></b> <b>(g)</b>	26.6	26.1	19.6#	26.9	25.6	18.1#	33.5	33.1	21.3#	32.7	33.5	22.1#
	±	±	±	±	±	±	±	±	±	±	±	±
	1.2	0.6	0.4	1.5	1.4	1.8	1.7	1.6	1.4	1.8	1.3	1.4
<b>Pt</b> <b>(g)</b>	3.8	4.3	4.2	4.8	4.3	4.9	7.1	7.5	5.6#	5.3	5.8	6.2
	±	±	±	±	±	±	±	±	±	±	±	±
	0.6	0.2	0.3	0.5	0.4	0.4	0.6	0.8	0.5	0.6	0.8	0.4

# Figure 1

a)



b)



c)

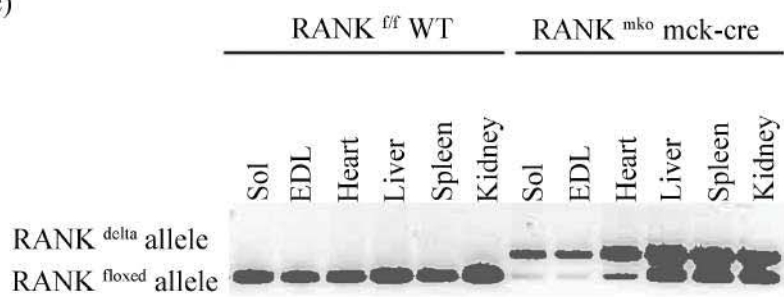


Figure 2

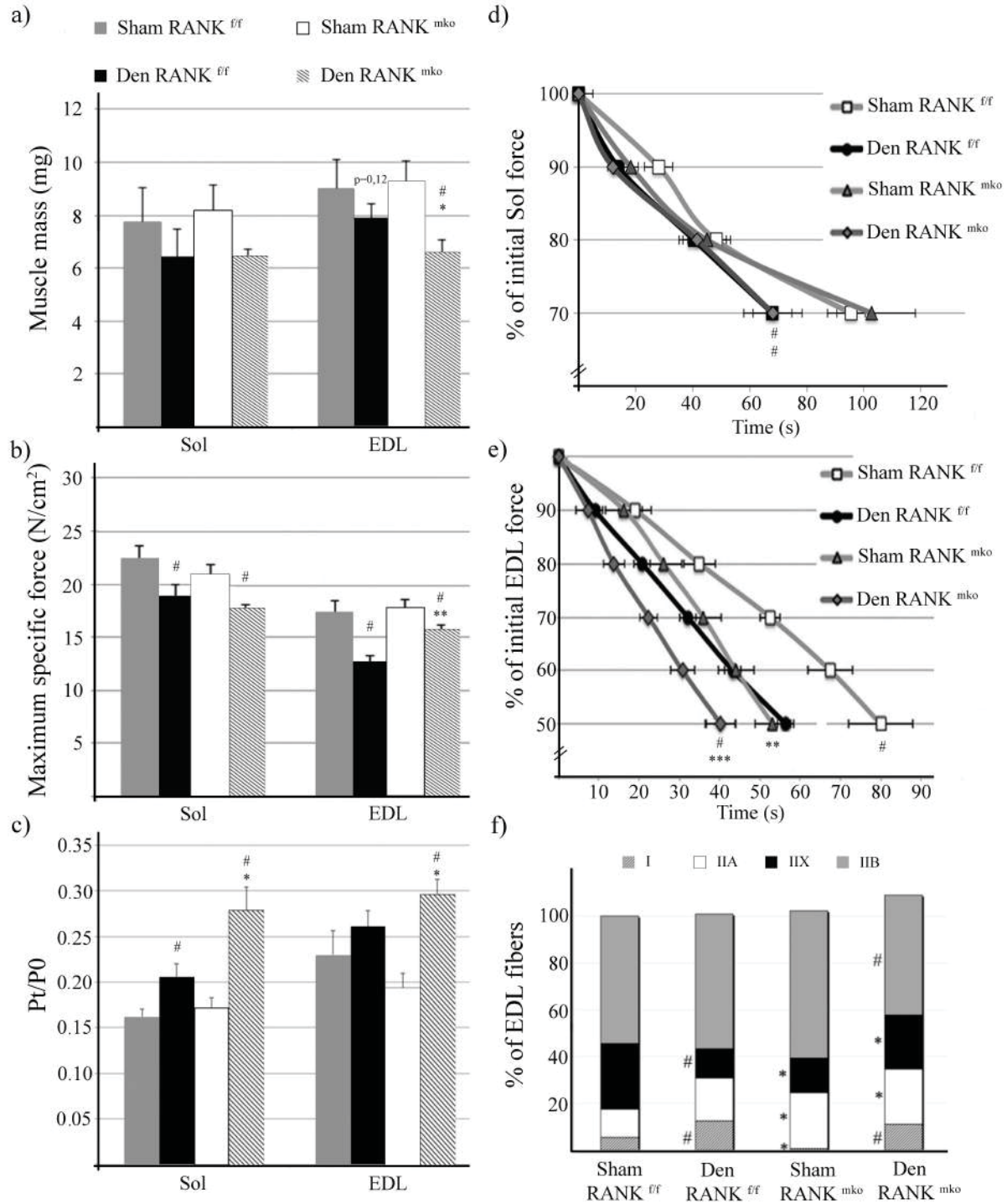
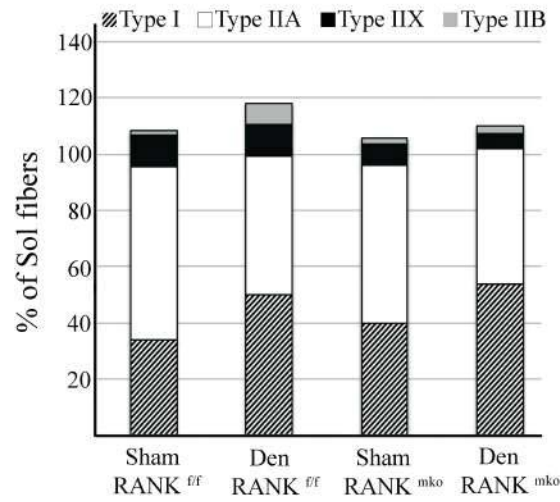




Figure 3

a)



b)

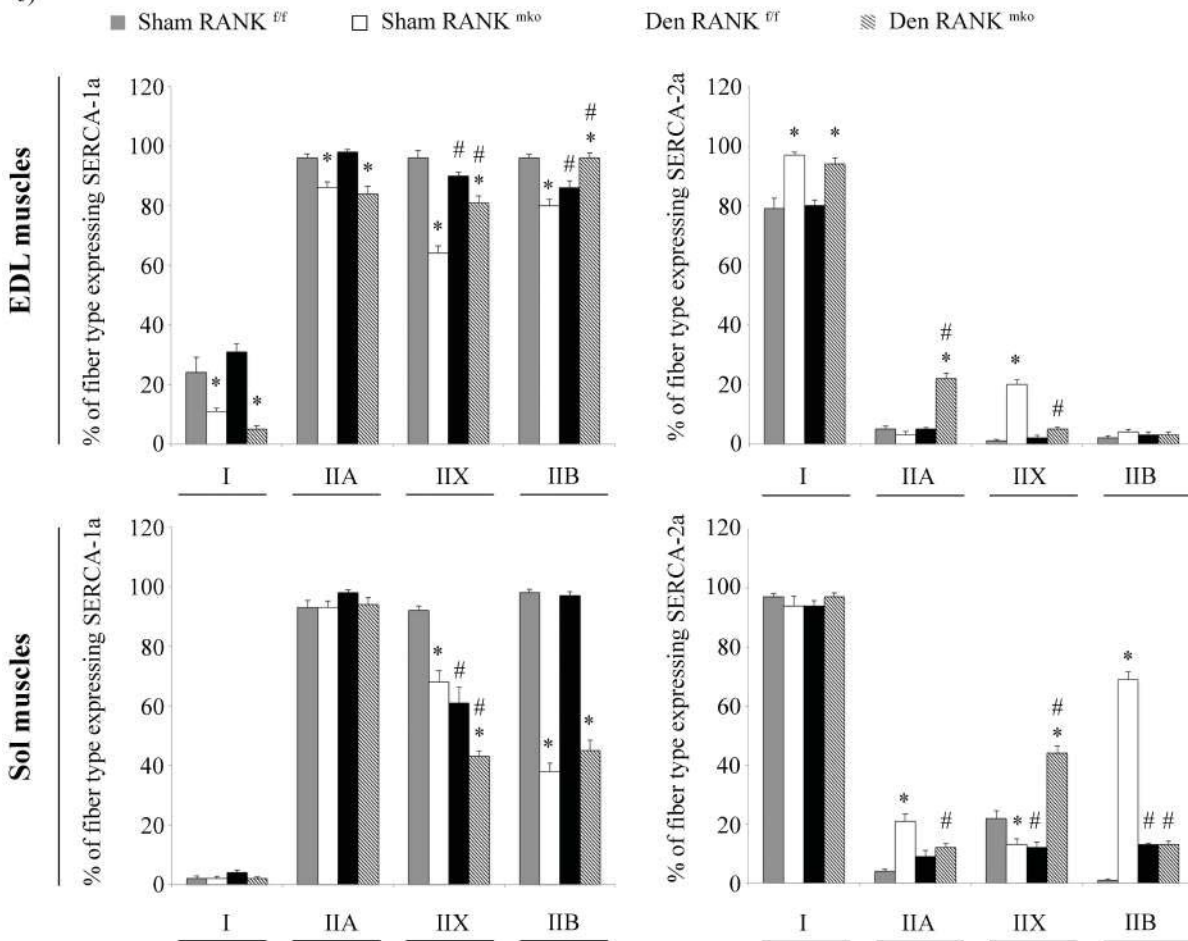


Figure 4

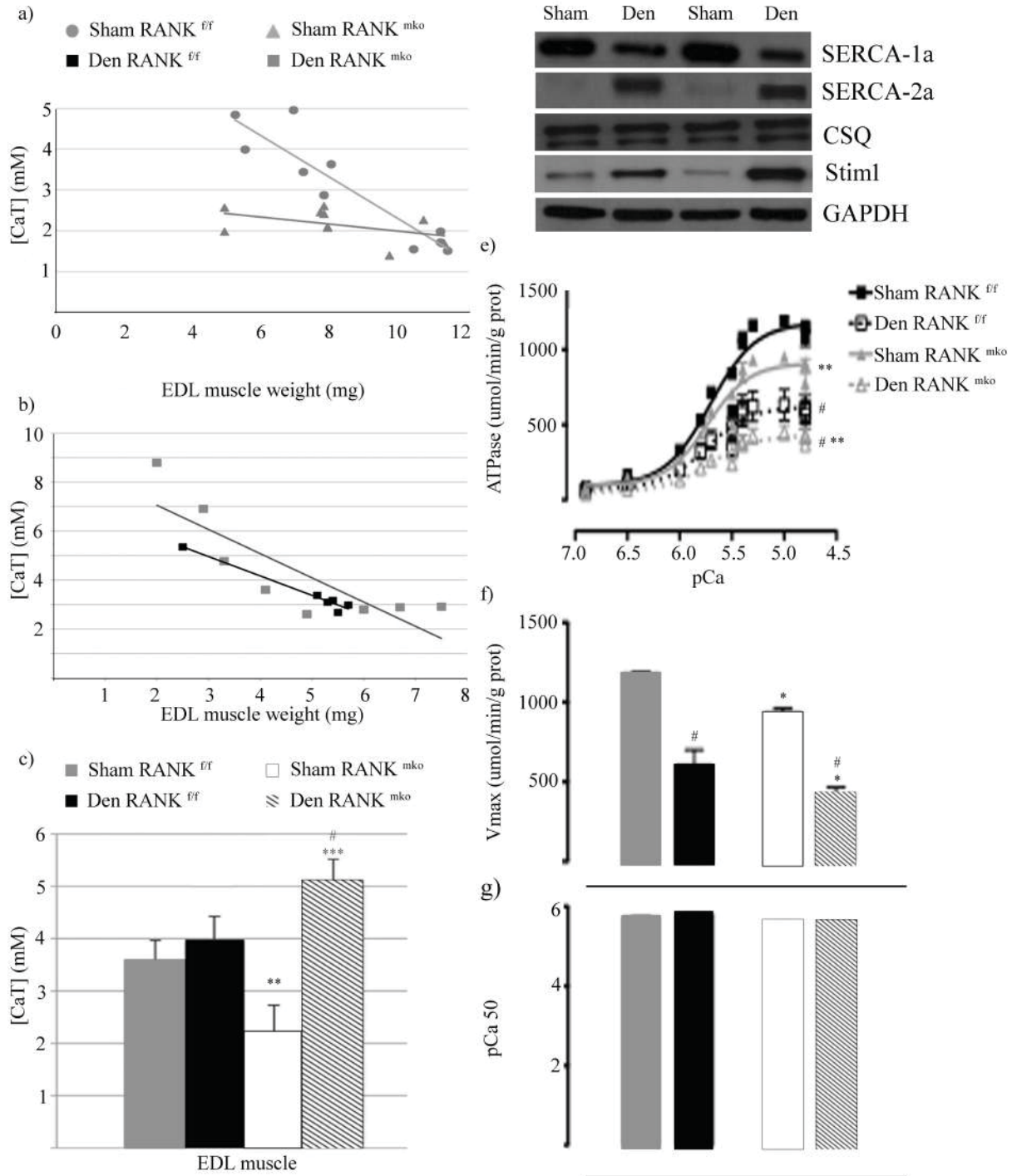


Figure 5

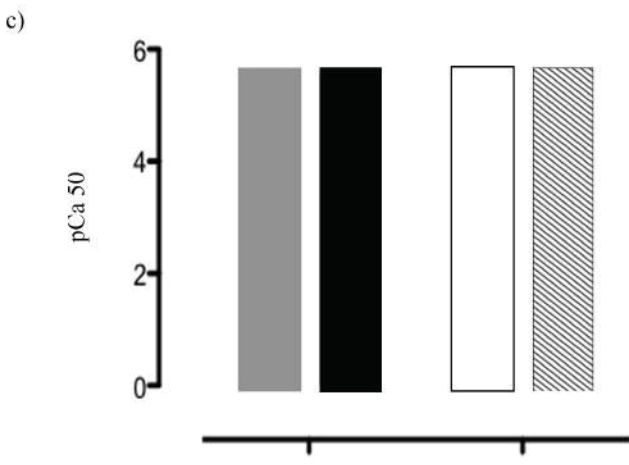
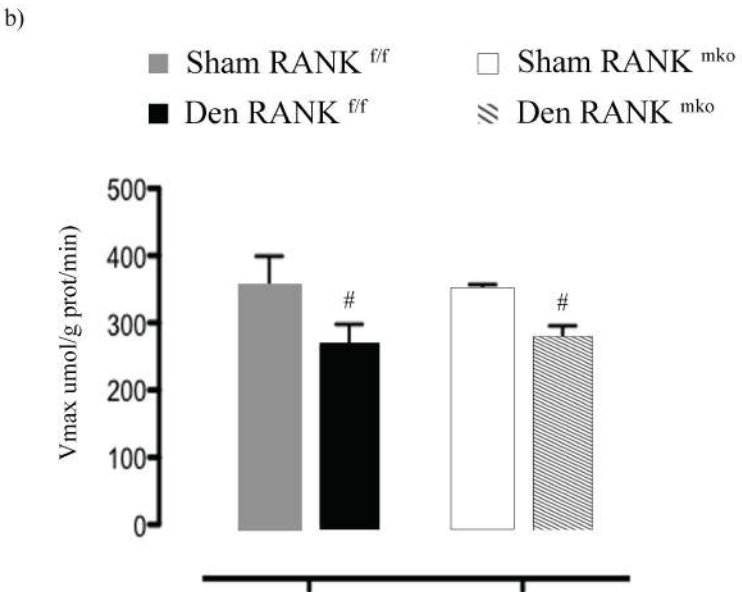
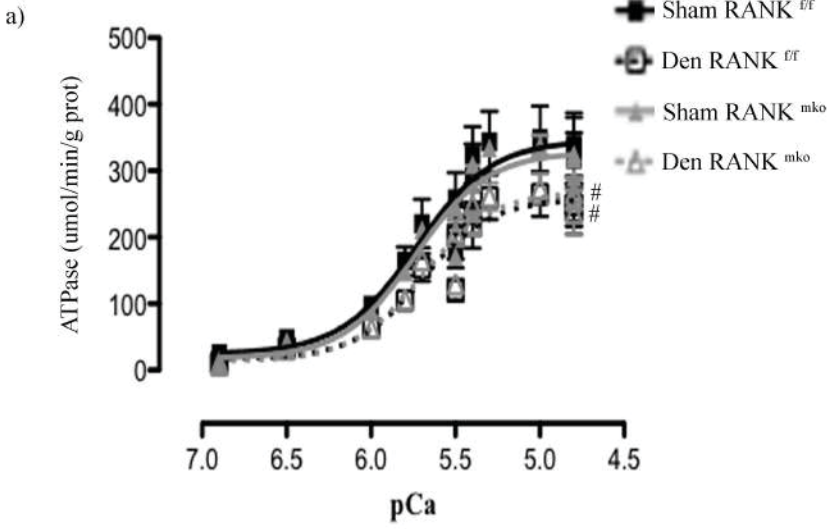


Figure 6

